

Centralized Energy-Efficient Multiuser Multiantenna Relaying in Next-Generation Radio Access Networks

Jiaxin Yang, *Student Member, IEEE*, Benoit Champagne, *Senior Member, IEEE*, Yulong Zou, *Senior Member, IEEE*, and Lajos Hanzo, *Fellow, IEEE*

Abstract—This paper addresses the design of a multiuser relaying subnetwork within a cloud radio access network (C-RAN) from an energy-efficient perspective. In the relaying subnetwork, multiple source–destination pairs communicate with the assistance of multiple remote radio heads (RRHs) connected to the baseband unit pool. Exploiting the flexible centralized processing structure of C-RAN, where RRHs can be adaptively activated/deactivated, we formulate the problem as a quality-of-service (QoS) based network energy minimization problem via joint RRH selection and relaying matrix optimization. Since the resultant optimization problem is nonconvex and mathematically challenging, we propose an iterative solution based on the concept of the re-weighted l_1 norm, along with a block-coordinate descent type algorithm. The active RRHs are then determined in a single attempt by thresholding a group sparsity pattern associated with the set of all RRH relaying matrices. To circumvent a potentially undesirable condition, where the selected subset of RRHs fails to simultaneously satisfy all the destination users' QoS levels, we conceive a UE admission control mechanism for overcoming the associated *infeasibility* problem. Our simulation results demonstrate the explicit benefits of the proposed design approach, which results in a significantly lower energy consumption of the relaying subnetwork than conventional cooperative relaying.

Index Terms—Cloud radio access network (C-RAN), energy efficiency, multiantenna, multiuser, nonconvex optimization, quality-of-service (QoS), relaying, remote radio head (RRH).

I. INTRODUCTION

THE proliferation of smart wireless devices, along with an increasing user demand for high data-rate applications, impose significant challenges on the design of future cellular networks. To address these issues, the ultra-dense deployment of access points (APs) for creating small cell networks has been recognized as an effective potential solution to complement the

traditional radio access network (RAN) architecture, along the evolutionary path towards fifth-generation (5G) networks [1]. Due to its high area spectral efficiency associated with an aggressive near-unity frequency reuse factor, inter-cell interference coordination relying on joint signal processing is considered a key enabling technique for these networks [2]. To enable the low-cost implementation of these sophisticated schemes, a novel centralized RAN architecture, namely the cloud radio access network (C-RAN) concept, has been proposed as a potential solution for 5G networks [3], [4].

In a typical C-RAN, the distributed APs of each cell, also termed as the remote radio heads (RRHs), are connected to a cloud-based centralized data processing center, termed as the baseband unit (BBU) pool, via high-bandwidth low-latency fronthaul links. In contrast to the conventional macro-cell base stations, the RRHs are only equipped with multi-antenna-aided radio frequency (RF) front-end circuitry and analog-to-digital (A/D) converters, while all baseband digital processing functionalities have been shifted to the BBU pool. Upon collecting the channel state information (CSI) and user traffic data across different cells, the BBU pool becomes capable of performing joint beamforming for inter-cell interference coordination. As compared to the traditional RAN, the low assembly and maintenance costs associated with the RRHs may lead to a significant reduction of the capital and operating expenditures, which is one of the ultimate goals of 5G networks. Despite the aforementioned benefits of C-RAN, this new architecture also raises issues from an energy efficiency perspective. Due to the large number of RRHs involved in interference coordination and signal transmission, the associated energy consumption across the network is considerably increased, which naturally translates into both higher operating overhead costs and detrimental environmental impacts. Hence, the financial incentive of using low-cost RRHs could easily be offset by these factors. It is therefore of paramount importance to take into account the energy efficiency in the study of C-RAN and to develop “green” RRH low-energy transmit solutions for environmental sustainability.

As compared to the conventional cellular network design, the C-RAN benefits from its flexible centralized processing structure and allows the RRHs to be adaptively switched on or off according to the temporal and spatial data traffic pattern of cellular users. Inspired by this fact, a so-called *group sparse* beamforming framework has been proposed for network energy minimization in a C-RAN downlink (DL) multicast scenario [5]. Capitalizing on the compressive sensing theory, a so-called

Manuscript received December 29, 2015; revised May 4, 2016 and January 19, 2017; accepted March 1, 2017. Date of publication March 3, 2017; date of current version September 15, 2017. This work was supported by a grant from the Natural Sciences and Engineering Research Council of Canada. The review of this paper was coordinated by Prof. C.-X. Wang.

J. Yang and B. Champagne are with the Department of Electrical and Computer Engineering, McGill University, Montreal, QC H3A 0E9, Canada (e-mail: jiaxin.yang@mail.mcgill.ca; benoit.champagne@mcgill.ca).

Y. Zou is with the School of Telecommunications and Information Engineering, Nanjing University of Posts and Telecommunications, Nanjing, Jiangsu 210003, China (e-mail: yulong.zou@njupt.edu.cn).

L. Hanzo is with the School of Electronics and Computer Science, University of Southampton, Southampton SO17 1BJ, U.K. (e-mail: lh@ecs.soton.ac.uk).

Color versions of one or more of the figures in this paper are available online at <http://ieeexplore.ieee.org>.

Digital Object Identifier 10.1109/TVT.2017.2677880

group sparsity pattern is associated with the set of beamforming vectors across all the RRHs and used for obtaining a sparse solution, where only a subset of the RRHs are activated at any instant. The effect of imperfect CSI has been considered in [6] under the same network setup and a robust version of the group sparse beamforming solution has also been proposed with the aid of semidefinite relaxation. The joint DL and uplink (UL) energy minimization problem for C-RAN has been studied in [7], where the UL receive beamforming problem is equivalently translated into a virtual DL problem by invoking the well-established UL-DL duality theory. In [8], sparse beamforming has been also applied in solving the network utility maximization problem under the nonlinear constraint posed by finite-capacity fronthaul links. Large-scale optimization methods for various signal processing problems in C-RAN are also summarized in [9]. Whilst most of the prior contributions focus on coordinated beamforming in both DL and UL C-RAN setups, the exploitation of RRHs as relays for further improving the network capacity and coverage has remained hitherto largely undisclosed (see, e.g., [10], [11] and references therein for a comprehensive review of system optimization for conventional relaying networks).

Against this background, we investigate the minimization of energy consumption of a multi-user relaying sub-network operating within a C-RAN cluster. Specifically, we consider a sub-network, where multiple source and destination pairs (also termed user equipment (UE) in LTE) communicate with each others by relying on the assistance of multiple cooperative RRHs connected to the BBU pool. Taking into account both the static (fixed circuitry) and dynamic (RF transmission) components of the RRHs power [12], a joint RRH selection as well as amplify-and-forward (AF) matrix design problem is formulated, whereby the total power consumption is minimized over the relaying sub-network while maintaining a predefined QoS level at each destination UE. To solve the resultant non-convex problem and to arrive at a sparse solution, an iterative approach relying on the concepts of re-weighted l_1 norm minimization [13] along with a block coordinate descent (BCD)-type update [14] is proposed. Following this optimization, the subset of active RRHs selected for relaying the transmission is determined in a single instance by thresholding the recovered group sparsity pattern vector. In addition, to overcome a potentially undesired scenario, where the sub-network fails to simultaneously satisfy all the destination UEs' QoS levels with the aid of only the selected subset of RRHs, we propose an iterative user admission control scheme. Explicitly, in this proposed scheme, specific destination UEs exhibiting a high "infeasibility indicator" will be excluded from the optimization procedure by the network for the sake of maintaining the QoS of all the other users. The quantitative benefits of the proposed joint design algorithm and admission control scheme are demonstrated by computer simulations.

The remainder of the paper is organized as follows. The relaying system model of the C-RAN is introduced in Section II. In Section III, we formulate and solve the network energy minimization problem. Furthermore, an iterative UE admission control mechanism is proposed for overcoming the potential infeasibility issue as mentioned above. Our simula-

tion results quantifying the benefits of the proposed algorithms are provided in Section IV. Finally, the paper is concluded in Section V.

II. SYSTEM MODEL

Consider a multi-user relaying sub-network within a C-RAN, consisting of L multi-antenna RRHs and K pairs of single-antenna source UEs (SUEs) and destination UEs (DUEs), as depicted in Fig. 1(a). The L RRHs work collaboratively under the C-RAN umbrella, relaying the messages of the SUEs to their corresponding DUEs. It is assumed that each SUE only communicates with its paired DUE. The RRHs and SUE-DUE pairs are indexed by the sets $\mathcal{L} \triangleq \{1, 2, \dots, L\}$ and $\mathcal{K} \triangleq \{1, 2, \dots, K\}$, respectively. For each $l \in \mathcal{L}$, RRH- l is equipped with N_l antennas and operates in a half-duplex AF mode. It is assumed that no direct links are available between the SUEs and DUEs due to a high pathloss.

We consider a narrowband flat-fading channel model, where $\mathbf{h}_{l,k} \in \mathbb{C}^{N_l \times 1}$ specifies the channel between SUE- k and RRH- l , while $\mathbf{g}_{k,m} \in \mathbb{C}^{N_l \times 1}$ denotes the Hermitian transpose of the channel between RRH- l and DUE- k . Let s_k denote the information symbol transmitted by SUE- k at a specific time instance, which is modeled as a zero-mean unit-variance complex random variable. During the first transmission phase, RRH- l receives the following signal:

$$\mathbf{r}_l = \sum_{k=1}^K \mathbf{h}_{l,k} s_k + \mathbf{n}_{R,l}, \quad l \in \mathcal{L} \quad (1)$$

where $\mathbf{n}_{R,l}(n)$ denotes the spatially white, additive noise vector at RRH- l with zero mean and covariance matrix $\sigma_{R,l}^2 \mathbf{I}_{N_l}$. During the second phase, for each $l \in \mathcal{L}$, RRH- l applies a linear transformation matrix $\mathbf{W}_l \in \mathbb{C}^{N_l \times N_l}$ to \mathbf{r}_l and forwards the resultant signal to all DUEs. The signal received by DUE- k can be expressed as

$$\begin{aligned} y_k &= \sum_{l=1}^L \mathbf{g}_{k,l}^H \mathbf{W}_l \mathbf{r}_l + n_{D,k} \\ &= \underbrace{\sum_{l=1}^L \mathbf{g}_{k,l}^H \mathbf{W}_l \mathbf{h}_{l,k} s_k}_{\text{Desired Signal}} + \underbrace{\sum_{l=1}^L \sum_{\substack{m=1, \\ m \neq k}}^K \mathbf{g}_{k,l}^H \mathbf{W}_l \mathbf{h}_{l,m} s_m}_{\text{Multi-User Interference}} \\ &\quad + \underbrace{\sum_{l=1}^L \mathbf{g}_{k,l}^H \mathbf{W}_l \mathbf{n}_{R,l}}_{\text{Noise Terms}} + n_{D,k}, \quad k \in \mathcal{K} \end{aligned} \quad (2)$$

where $n_{D,k}$ denotes the additive white noise at DUE- k with zero mean and a variance of $\sigma_{D,k}^2$. The above expression indicates that the signal received at each DUE is a superposition of the desired signal component, the multi-user interference (co-channel interference) arriving from the other SUEs as well as the noise contributions from the RRHs and the DUE. This general interference scenario, which is illustrated in Fig. 1(b), is often referred to as the relay-aided interference channel in the literature of

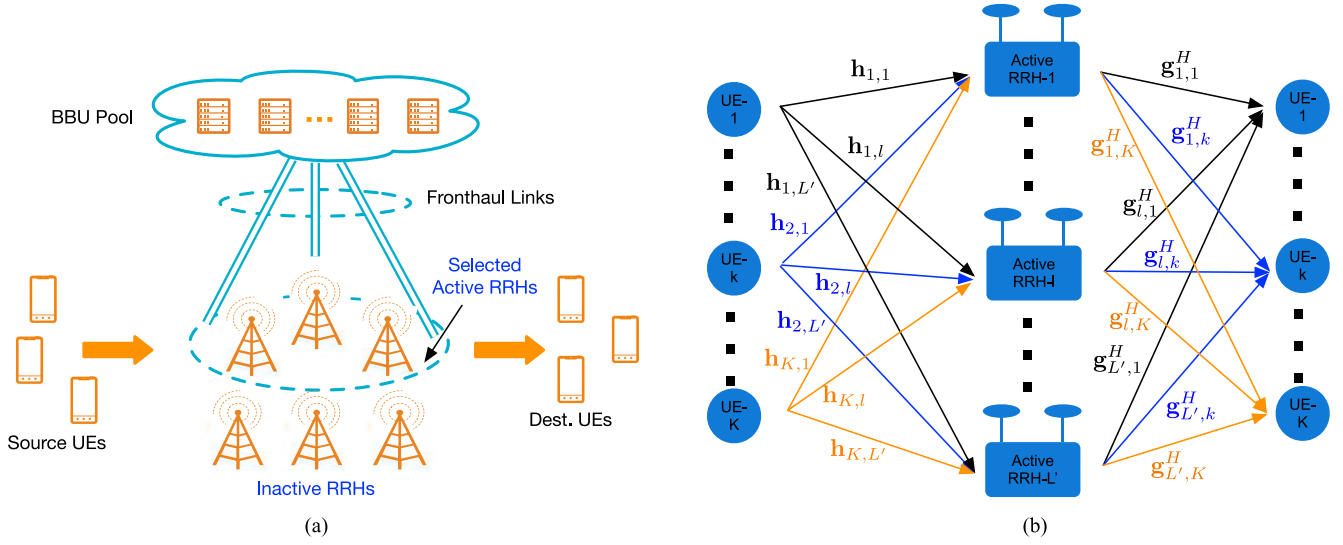


Fig. 1. Multi-user multi-relay sub-network within a C-RAN and illustration of the interference scenario within the sub-network. (a) Multi-user relaying sub-network within a C-RAN. (b) Interference scenario (L' denotes the number of active RRHs).

relaying optimization [15]–[19] and of interference alignment [20], [21].

We rely on the mean-square error (MSE) as the QoS metric for the received signal of each DUE. After DUE- k applies an equalizer gain u_k to its received signal y_k , resulting in the soft estimate \hat{s}_k , i.e., $\hat{s}_k = u_k^* y_k$, the MSE at DUE- k can be expressed as

$$\begin{aligned} \text{MSE}_k(u_k, \{\mathbf{W}_l\}) &= \mathbb{E} \{ |u_k^* y_k - s_k|^2 \} \\ &= \sum_{q=1}^K \left| \sum_{l=1}^L \mathbf{g}_{k,l}^H \mathbf{W}_l \mathbf{h}_{l,q} \right|^2 |u_k|^2 - \sum_{l=1}^L 2\Re \{ u_k^* \mathbf{g}_{k,l}^H \mathbf{W}_l \mathbf{h}_{l,k} \} \\ &\quad + \sum_{l=1}^L \sigma_{R,l}^2 \|\mathbf{g}_{k,l}^H \mathbf{W}_l\|_2^2 |u_k|^2 + \sigma_{D,k}^2 |u_k|^2 + 1. \end{aligned} \quad (3)$$

The transmission power required for AF relaying at RRH- l is given by

$$P_{t,l} = \text{Tr} \left(\mathbf{W}_l^H (\sigma_{R,l}^2 \mathbf{I}_{N_l} + \sum_{k=1}^K \mathbf{h}_{l,k} \mathbf{h}_{l,k}^H) \mathbf{W}_l \right). \quad (4)$$

In addition to the transmission power, we also consider the static power consumption associated with each RRH, including that of the RF circuitry, A/D conversion and optical fronthaul. This power, which is non-negligible, can be saved when the associated RRH is switched off [5]–[7]. Denoting the static power level of RRH- l by $P_{c,l}$, the total relaying sub-network power consumption is given by

$$P = \sum_{l=1}^L \mathcal{I}(\|\mathbf{W}_l\|_F^2) P_{c,l} + \sum_{l=1}^L P_{t,l}, \quad (5)$$

where $\mathcal{I}(\cdot)$ denotes the indicator function, i.e., $\mathcal{I}(x) = 1$ if $x \neq 0$ and $\mathcal{I}(x) = 0$, otherwise. Based on (3) and (5), we then formulate the energy minimization problem with QoS constraints in the next section.

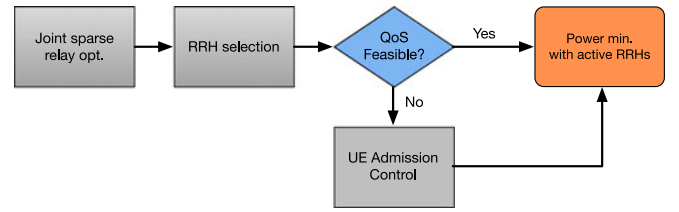


Fig. 2. Overall flow of the proposed algorithm.

III. ENERGY MINIMIZATION DESIGN AND UE ADMISSION CONTROL

In this section, we first develop an energy-efficient multi-user relaying solution for C-RAN by jointly optimizing the relay AF matrices $\{\mathbf{W}_l\}$ at all RRHs and performing RRH selection. To circumvent the undesirable condition where the DUEs' QoS levels cannot all be simultaneously satisfied by the selected subset of RRHs, we will also propose a UE admission control mechanism for overcoming the associated *infeasibility* problem. The overall flow of the proposed solution is depicted in Fig. 2, which consists of the following main steps:

- Optimize the AF relaying matrices across all RRHs by introducing a sparsity-inducing l_1 -norm.
- Perform RRH selection by exploiting the group sparsity pattern obtained from the first step.
- If the above-mentioned infeasibility problem is observed, involve the UE admission control algorithm.

A. Iterative Algorithm

We first aim for minimizing the total energy consumption of the relaying sub-network by simultaneously designing the AF matrices $\{\mathbf{W}_l\}$ for all the RRHs and the equalizer gains $\{u_k\}$ for all the DUEs, while still maintaining a predefined QoS level at each DUE. To connect this problem to the vast body of literature on sparse signal recovery [22], we express the indicator function

$\mathcal{I}(\cdot)$ in (5) in terms of the l_0 -norm $\|\cdot\|_0$. The design problem can then be mathematically expressed as¹

$$\min_{\mathbf{u}, \{\mathbf{W}_l\}} \sum_{l=1}^L \|\|\mathbf{W}_l\|_F^2\|_0 P_{c,l} + \sum_{l=1}^L P_{t,l} + \|\mathbf{u}\|_2^2 \quad (6a)$$

$$\text{s.t. } \text{MSE}_k(u_k, \{\mathbf{W}_l\}) \leq \gamma_k \quad \forall k \in \mathcal{K} \quad (6b)$$

$$P_{t,l} \leq P_{l,\max} \quad \forall l \in \mathcal{L} \quad (6c)$$

where γ_k denotes the predefined target MSE of DUE- k and $\mathbf{u} = [u_1, \dots, u_K]^T$.

To overcome the non-convexity issues of (6a) due to the l_0 -norm, we follow a similar approach as in [13] and use the so-called re-weighted l_1 -norm minimization for approximating the non-convex l_0 -norm. Specifically, this approach yields $\|\|\mathbf{W}_l\|_F^2\|_0 \approx \frac{\mu}{\|\mathbf{W}_l^{(n-1)}\|_F^2 + \varepsilon} \|\mathbf{W}_l\|_F^2$, where $\mathbf{W}_l^{(n-1)}$ denotes the value of \mathbf{W}_l from a previous iteration (with index $n-1$), μ is a positive constant (to be specified later) and $\varepsilon > 0$ is a small positive constant ensuring numerical stability. Using the latter approximation, (6) can be reformulated as:

$$\min_{\mathbf{u}, \{\mathbf{W}_l\}} \sum_{l=1}^L \frac{\mu}{\|\mathbf{W}_l^{(n-1)}\|_F^2 + \varepsilon} \|\mathbf{W}_l\|_F^2 P_{c,l} + \sum_{l=1}^L P_{t,l} + \|\mathbf{u}\|_2^2 \quad (7a)$$

$$\text{s.t. } \text{MSE}_k(u_k, \{\mathbf{W}_l\}) \leq \gamma_k \quad \forall k \in \mathcal{K} \quad (7b)$$

$$P_{t,l} \leq P_{l,\max} \quad \forall l \in \mathcal{L}. \quad (7c)$$

However, after this approximation, the above problem still remains non-convex due to the fact that the variables $\{u_k\}$ and $\{\mathbf{W}_l\}$ are nonlinearly coupled in the QoS constraints (7b). Then, a further inspection of the MSE expression (3) reveals that it has a so-called bi-convex structure, i.e., it is convex with respect to one block of variables when the other is fixed. Based on this property, we can solve the problem by employing the BCD-type algorithm of [23], which makes it possible to update the two blocks of variables one at a time while fixing the values of the other. In this way, (7) can be solved iteratively with respect to \mathbf{u} and $\{\mathbf{W}_l\}$ in Gauss-Seidel fashion. Below, we formulate the two sub-problems and derive their corresponding solutions.

1) *Updating \mathbf{u}* : With fixed AF relaying matrices $\{\mathbf{W}_l\}$, the sub-problem solution of finding the optimal \mathbf{u}^{opt} can be expressed as

$$\min_{\mathbf{u}} \|\mathbf{u}\|_2^2 \quad (8a)$$

$$\text{s.t. } \text{MSE}_k(u_k) \leq \gamma_k \quad \forall k \in \mathcal{K}. \quad (8b)$$

¹The addition of the term $\|\mathbf{u}\|_2^2$ in the objective function (6a) makes the latter strongly convex in \mathbf{u} . This modification does not affect the feasibility of the problem, i.e., the feasible set $\mathcal{F} = \{(\mathbf{u}, \{\mathbf{W}_l\}) : (6b), (6c)\}$ remains unchanged. More importantly, the strong convexity of (6a) is useful in ensuring the convergence of the algorithm derived subsequently.

Noting the separable structure of the above problem with respect to u_1, \dots, u_K , it can be further decomposed into K parallel sub-problems given by

$$\min_{u_k} |u_k|^2 \quad (9a)$$

$$\text{s.t. } \sum_{q=1}^K \left| \sum_{l=1}^L \mathbf{g}_{k,l}^H \mathbf{W}_l \mathbf{h}_{l,q} \right|^2 |u_k|^2 - \sum_{l=1}^L 2\Re \{u_k^* \mathbf{g}_{k,l}^H \mathbf{W}_l \mathbf{h}_{l,k}\} + \sum_{l=1}^L \sigma_{R,l}^2 \|\mathbf{g}_{k,l}^H \mathbf{W}_l\|_2^2 |u_k|^2 + \sigma_{D,k}^2 |u_k|^2 + 1 \leq \gamma_k. \quad (9b)$$

Below we show that the optimal solution u_k^{opt} of (9) in fact can be obtained as a scaled version of the MMSE filter u_k^{MMSE} . Observe that (9) is a strictly convex quadratic problem, which is also strictly feasible, i.e., Slater's constraint qualification holds [24]. Therefore, there exists a unique globally optimal solution of (9), which can be obtained by evaluating the Karush-Kuhn-Tucker (KKT) conditions of (9), which are sufficient conditions in this case. First, the Lagrangian function of (9) can be written as

$$\begin{aligned} \mathcal{L}(u_k, \mu_k) &= |u_k|^2 + \mu_k \left(\sum_{q=1}^K \left| \sum_{l=1}^L \mathbf{g}_{k,l}^H \mathbf{W}_l \mathbf{h}_{l,q} \right|^2 |u_k|^2 \right. \\ &\quad - \sum_{l=1}^L 2\Re \{u_k^* \mathbf{g}_{k,l}^H \mathbf{W}_l \mathbf{h}_{l,k}\} \\ &\quad + \sum_{l=1}^L \sigma_{R,l}^2 \|\mathbf{g}_{k,l}^H \mathbf{W}_l\|_2^2 |u_k|^2 \\ &\quad \left. + \sigma_{D,k}^2 |u_k|^2 + 1 - \gamma_k \right) \end{aligned} \quad (10)$$

where $\mu_k \geq 0$ denotes the dual variable associated with (9b). The first-order KKT condition can then be formulated as

$$\begin{aligned} \frac{\partial \mathcal{L}(u_k, \mu_k)}{\partial u_k^*} &= u_k \left(\mu_k \sum_{q=1}^K \left| \sum_{l=1}^L \mathbf{g}_{k,l}^H \mathbf{W}_l \mathbf{h}_{l,q} \right|^2 + \mu_k \sum_{l=1}^L \sigma_{R,l}^2 \|\mathbf{g}_{k,l}^H \mathbf{W}_l\|_2^2 \right. \\ &\quad \left. + \mu_k \sigma_{D,k}^2 + 1 \right) - \mu_k \sum_{l=1}^L \mathbf{g}_{k,l}^H \mathbf{W}_l \mathbf{h}_{l,k} = 0. \end{aligned} \quad (11)$$

Re-arranging the above, we obtain u_k^{opt} (12), shown bottom of the page.

Meanwhile, the MMSE filter can be obtained by setting the partial derivative of $\text{MSE}_k(u_k)$ in (3) to zero, yielding

$$u_k^{\text{opt}} = \frac{\mu_k \sum_{l=1}^L \mathbf{g}_{k,l}^H \mathbf{W}_l \mathbf{h}_{l,k}}{\mu_k \left(\sum_{q=1}^K \left| \sum_{l=1}^L \mathbf{g}_{k,l}^H \mathbf{W}_l \mathbf{h}_{l,q} \right|^2 + \sum_{l=1}^L \sigma_{R,l}^2 \|\mathbf{g}_{k,l}^H \mathbf{W}_l\|_2^2 + \sigma_{D,k}^2 \right) + 1}. \quad (12)$$

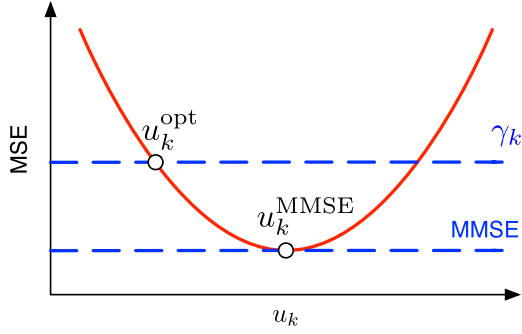


Fig. 3. How to obtain the optimal u_k^* from the MMSE solution u_k^{MMSE} .

$\frac{\partial \text{MSE}_k(u_k)}{\partial u_k^*} = 0$, whose solution is

$$u_k^{\text{MMSE}} = \frac{\sum_{l=1}^L \mathbf{g}_{k,l}^H \mathbf{W}_l \mathbf{h}_{l,k}}{\sum_{q=1}^K \left| \sum_{l=1}^L \mathbf{g}_{k,l}^H \mathbf{W}_l \mathbf{h}_{l,q} \right|^2 + \sum_{l=1}^L \sigma_{\text{R},l}^2 \|\mathbf{g}_{k,l}^H \mathbf{W}_l\|_2^2 + \sigma_{\text{D},k}^2} \quad (13)$$

Upon dividing (13) by (12), we obtain

$$\frac{u_k^{\text{MMSE}}}{u_k^{\text{opt}}} = \frac{\mathcal{C} + \frac{1}{\mu_k}}{\mathcal{C}} \quad (14)$$

where $\mathcal{C} = \sum_{q=1}^K \left| \sum_{l=1}^L \mathbf{g}_{k,l}^H \mathbf{W}_l \mathbf{h}_{l,q} \right|^2 + \sum_{l=1}^L \sigma_{\text{R},l}^2 \|\mathbf{g}_{k,l}^H \mathbf{W}_l\|_2^2 + \sigma_{\text{D},k}^2$ is a positive constant given fixed $\{\mathbf{W}_l\}$. Upon defining $\kappa_k = 1 + \frac{1}{\mathcal{C}\mu_k} > 1$, we now recognize that u_k^{opt} can be found by scaling down the MMSE filter u_k^{MMSE} by κ_k as follows:

$$\begin{aligned} u_k^{\text{opt}} &= \frac{u_k^{\text{MMSE}}}{\kappa_k} \\ &= \frac{1}{\kappa_k} \\ &\times \frac{\sum_{l=1}^L \mathbf{g}_{k,l}^H \mathbf{W}_l \mathbf{h}_{l,k}}{\sum_{q=1}^K \left| \sum_{l=1}^L \mathbf{g}_{k,l}^H \mathbf{W}_l \mathbf{h}_{l,q} \right|^2 + \sum_{l=1}^L \sigma_{\text{R},l}^2 \|\mathbf{g}_{k,l}^H \mathbf{W}_l\|_2^2 + \sigma_{\text{D},k}^2} \end{aligned} \quad (15)$$

To gain more insights into the computation of u_k^{opt} , we illustrate the relationship between u_k^{opt} and the MMSE filter u_k^{MMSE} in Fig. 3, where for simplicity, we assume that u_k is real-valued. Since $\text{MSE}_k(u_k)$ is a quadratic function in u_k , we can first compute the global minimum, i.e., the MMSE solution u_k^{MMSE} , and then simply scaling it down by a factor κ_k while still satisfying the MSE constraint (8b), i.e., letting $\text{MSE}_k(u_k) = \gamma_k$.

2) *Updating $\{\mathbf{W}_l\}$* : We then proceed to solve the sub-problem for $\{\mathbf{W}_l\}$ when \mathbf{u} is fixed. To this end, we define the concatenated weight vectors $\mathbf{w}_l \triangleq \text{vec}(\mathbf{W}_l)$ for all l , as well as the following matrices and vectors, which are independent of

$\{\mathbf{w}_l\}$:

$$\mathbf{Q}_{l,m}^k = \sum_{q=1}^K (\mathbf{h}_{l,q}^* u_k u_k^* \mathbf{h}_{l,q}^T \otimes \mathbf{g}_{q,l} \mathbf{g}_{q,l}^H) \quad (16)$$

$$\mathbf{\Psi}_l = \sigma_{\text{R},l}^2 \mathbf{I}_{N_l^2} + \mathbf{I}_{N_l} \otimes \sum_{k=1}^K \mathbf{h}_{l,k} \mathbf{h}_{l,k}^H \quad (17)$$

$$\mathbf{\Theta}_{k,l} = \sigma_{\text{R},l}^2 \mathbf{I} \otimes (\mathbf{g}_{k,l} u_k u_k^* \mathbf{g}_{k,l}^H) \quad (18)$$

$$\mathbf{q}_{k,l} = \mathbf{h}_{l,k}^* \otimes \mathbf{g}_{k,l}. \quad (19)$$

Then, by exploiting the useful properties of the Kronecker product, i.e., $\text{Tr}(\mathbf{A}^H \mathbf{B} \mathbf{C} \mathbf{D}^H) = \text{vec}(\mathbf{A})^H (\mathbf{D}^T \otimes \mathbf{B}) \text{vec}(\mathbf{C})$, $\text{Tr}(\mathbf{A}^H \mathbf{B} \mathbf{A}) = \text{vec}(\mathbf{A})^H (\mathbf{I} \otimes \mathbf{B}) \text{vec}(\mathbf{A})$ and $\text{Tr}(\mathbf{A}^H \mathbf{B}) = \text{vec}(\mathbf{B})^H \text{vec}(\mathbf{A})$, we arrive at the following convex quadratic constrained quadratic problem (QCQP):

$$\min_{\mathbf{w}} \sum_{l=1}^L \frac{\mu}{\|\mathbf{w}_l^{(n-1)}\|_2^2 + \varepsilon} \|\mathbf{w}_l\|_2^2 P_{c,l} + \sum_{l=1}^L \mathbf{w}_l^H \mathbf{\Psi}_l \mathbf{w}_l \quad (20a)$$

$$\text{s.t.} \quad \sum_{l=1}^L \sum_{m=1}^L \mathbf{w}_l^H \mathbf{Q}_{l,m}^k \mathbf{w}_m - \sum_{l=1}^L 2\Re\{\mathbf{w}_l^H \mathbf{q}_{k,l}\} \quad (20b)$$

$$+ \sum_{l=1}^L \mathbf{w}_l^H \mathbf{\Theta}_{k,l} \mathbf{w}_l + q_k \leq \gamma_k \quad \forall k \in \mathcal{K} \quad (20b)$$

$$\mathbf{w}_l^H \mathbf{\Psi}_l \mathbf{w}_l \leq P_{l,\max} \quad \forall l \in \mathcal{L}. \quad (20c)$$

The class of problems in the above form can be equivalently transformed into a second-order cone program (SOCP) using the techniques introduced in [25]. To elaborate further, we first recast (20b) as

$$\mathbf{w}^H \mathbf{Q}_k \mathbf{w} - 2\Re\{\mathbf{w}^H \mathbf{q}_k\} + \mathbf{w}^H \mathbf{\Theta} \mathbf{w} + q_k - \gamma_k \leq 0, \quad (21)$$

where $\mathbf{q}_k \triangleq [\mathbf{q}_{k,1}^T, \dots, \mathbf{q}_{k,L}^T]^T$, $\mathbf{\Theta} \triangleq \text{blkdiag}\{\mathbf{\Theta}_1, \dots, \mathbf{\Theta}_L\}$ and \mathbf{Q}_k is a block matrix with its $(l, m)^{\text{th}}$ blocked given by $\mathbf{Q}_{l,m}^k$. With the aid of (21), (20) can further be reformulated as

$$\min_{\mathbf{w}, t_1, t_2, t_3, t_4} \sum_{l=1}^L \frac{\mu P_{c,l}}{\|\mathbf{w}_l^{(n-1)}\|_2^2 + \varepsilon} t_{1,l} + \sum_{l=1}^L t_{2,l} \quad (22a)$$

$$\text{s.t.} \quad t_{3,k}^2 + t_4^2 - \mathbf{q}_k \mathbf{Q}_k^{-1} \mathbf{q}_k + q_k - \gamma_k \leq 0 \quad \forall k \in \mathcal{K} \quad (22b)$$

$$t_{2,l} \leq P_{l,\max} \quad \forall l \in \mathcal{L} \quad (22c)$$

$$\|\mathbf{w}_l\|_2^2 \leq t_{1,l} \quad \forall l \in \mathcal{L} \quad (22d)$$

$$\|\mathbf{\Psi}_l^{1/2} \mathbf{w}_l\|_2^2 \leq t_{2,l} \quad \forall l \in \mathcal{L} \quad (22e)$$

$$\|\mathbf{Q}_k^{1/2} \mathbf{w} - \mathbf{Q}_k^{-1/2} \mathbf{q}_k\|_2^2 \leq t_{3,k} \quad \forall k \in \mathcal{K} \quad (22f)$$

$$\|\mathbf{\Theta}^{1/2} \mathbf{w}\|_2^2 \leq t_4 \quad (22g)$$

where $\mathbf{t}_1 = [t_{1,1}, \dots, t_{1,L}]^T$, $\mathbf{t}_2 = [t_{2,1}, \dots, t_{2,L}]^T$, $\mathbf{t}_3 = [t_{3,1}, \dots, t_{3,K}]^T$ and t_4 are auxiliary variables. It is observed that the objective function (22a) and the constraint (22c) are linear while (22f)–(22g) are in the form of second-order cones (SOCs). The remaining difficulties in solving (22) lie in (22b),

Algorithm 1: Re-weighted iterative algorithm for energy minimization using BCD update.

Initialization: $\mathbf{w}_l^{(0)}$ and $\beta_l = \frac{1}{\|\mathbf{w}_l^{(0)}\|_2^2 + \epsilon}$ for all $l \in \mathcal{L}$;

repeat

- 1) Update $u_k^{(n)}$ for all k in parallel via (15) given fixed $\mathbf{W}_l = \text{dvec}(\mathbf{w}_l^{(n-1)})$ for all l ;
- 2) Update $\mathbf{w}_l^{(n)}$ by solving the SOCP (22) with fixed $u_k = u_k^{(n)}$ for all k ;
- 3) Update the weight $\beta_l = \frac{1}{\|\mathbf{w}_l^{(n)}\|_2^2 + \epsilon}$ for all l .

until convergence;

Output: $(\bar{\mathbf{w}}, \bar{\mathbf{u}})$

(22d) and (22e), which are the so-called hyperbolic constraints [25]. To handle these constraints, we observe that for vector $\mathbf{x} \in \mathbb{C}^N$ and real scalars $y, z \geq 0$:

$$\|\mathbf{x}\|_2^2 \leq yz \iff \left\| \begin{bmatrix} 2\mathbf{x} \\ y - z \end{bmatrix} \right\|_2 \leq y + z. \quad (23)$$

As a direct application of (23), (22b), (22d), and (22e) can be respectively reformulated as

$$\left\| \begin{bmatrix} 2t_{3,k} \\ 2t_4 \\ \gamma_k - q_k + \mathbf{q}_k \mathbf{Q}_k^{-1} \mathbf{q}_k - 1 \end{bmatrix} \right\|_2 \leq \gamma_k - q_k + \mathbf{q}_k \mathbf{Q}_k^{-1} \mathbf{q}_k + 1 \quad (24)$$

$$\left\| \begin{bmatrix} 2\mathbf{w}_l \\ t_{1,l} - 1 \end{bmatrix} \right\|_2 \leq t_{1,l} + 1 \quad (25)$$

$$\left\| \begin{bmatrix} 2\Psi_l^{1/2} \mathbf{w}_l \\ t_{2,l} - 1 \end{bmatrix} \right\|_2 \leq t_{2,l} + 1. \quad (26)$$

Substituting the above inequalities back into (22), the latter becomes a standard SOCP, which can then be efficiently solved by interior-point methods. To this end, one can rely on state-of-the-art external software tools, see, e.g. [26].

With the aid of (15) and (22), the resultant iterative algorithm relying on the BCD and re-weighted l_1 -norm approximation can be now summarized as seen in Algorithm 1, where $\text{dvec}(\cdot)$ denotes the matrix-vector reshaping.

Remark 1: The design approach considered for our multi-user relay network is conceptually similar to that of [5] conceived for multi-cell downlink network, based on the QoS-constrained network power minimization. However, apart from the consideration of the different network topologies, the main difference between [5] and the present paper is the choice of QoS metric, which inevitably leads to different solution approaches. In [5], the signal-to-noise-plus-interference (SINR)-based constraints are imposed for the sake of guaranteeing a specific QoS level for each destination user. The SINR constraints can be equivalently written as an SOC constraint by applying a phase rotation (see [5, eq. (10)]), and therefore, the sub-problem at each iteration of the iterative algorithm is a convex SOCP. By contrast, in this paper, we adopt the MSE (3) as our QoS met-

ric, which is not jointly convex in $(\mathbf{u}, \{\mathbf{W}\}_l)$. This fundamental difference subsequently leads to a different iterative algorithm from that of [5], i.e., the so-called *block coordinate re-weighted l_1 -norm minimization*. Furthermore, in the context of the energy minimization problem considered, the convergence results of the conventional BCD algorithm [27]–[32] are not directly applicable to the proposed algorithm. In view of this, as an additional contribution, we show below the convergence properties of the newly proposed algorithm by relying on a proposition, which has only been discovered with the advent of recent advances in the non-convex optimization theory [23]. ■

B. Convergence Behavior

Since the original energy minimization problem of (6) is non-convex, it is necessary to analyze the convergence properties of Algorithm 1. Before proceeding further, let us take a closer look at the problem (6) in order to gain further insights into the proposed iterative algorithm. Similarly to the compressive sensing literature [13], we can approximate the l_0 -norm term of (6a) by a concave function as follows:

$$\begin{aligned} \sum_{l=1}^L \|\mathbf{W}_l\|_F^2 \|P_{c,l}\|_0 &= \sum_{l=1}^L \|\mathbf{w}_l\|_2^2 \|P_{c,l}\|_0 \\ &\approx \underbrace{\lambda_d \sum_{l=1}^L \log(1 + \|\mathbf{w}_l\|_2^2 \epsilon^{-1})}_{\mathcal{F}(\mathbf{w})} P_{c,l} \end{aligned} \quad (27)$$

where $\mathbf{w} = [\mathbf{w}_1^T, \dots, \mathbf{w}_L^T]^T$ and $\lambda_d = \frac{1}{\log(1 + \epsilon^{-1})}$. Then consider the following problem instead of (6):

$$\min_{(\mathbf{w}, \mathbf{u}) \in \Omega} \mathcal{F}'(\mathbf{w}, \mathbf{u}) \triangleq \mathcal{F}(\mathbf{w}) + \sum_{l=1}^L \mathbf{w}_l^H \Psi_l \mathbf{w}_l + \mathbf{u}^H \mathbf{u} \quad (28)$$

where for notational simplicity, we have $\Omega = \{(\mathbf{w}, \mathbf{u}) : (6b), (6c)\}$. Since $\mathcal{F}(\cdot)$ is concave, an efficient technique of solving (28) is the so-called majorization minimization (MM) algorithm [33]. The idea behind the MM algorithm is to first find a convex surrogate function, which majorizes the objective function and subsequently solves the original problem iteratively via a sequence of “convexified” sub-problems.

In (28), $\mathcal{F}(\cdot)$ is the only non-convex part, whose majorization function can simply be constructed from its first-order Taylor series expansion around a solution point $\mathbf{w}^{(n-1)}$ obtained from the previous iteration, i.e.,

$$\begin{aligned} \tilde{\mathcal{F}}(\mathbf{w}; \mathbf{w}^{(n-1)}) &= \mathcal{F}(\mathbf{w}^{(n-1)}) \\ &+ \lambda_d \sum_{l=1}^L \frac{\|\mathbf{w}_l\|_2 - \|\mathbf{w}_l^{(n-1)}\|_2}{\|\mathbf{w}_l^{(n-1)}\|_2 + \epsilon} \geq \mathcal{F}(\mathbf{w}). \end{aligned} \quad (29)$$

Then a modified block-type MM algorithm can be obtained for (28) by solving the following pair of sub-problems in a

circular manner:

$$\text{Step 1) } \mathbf{w}^{(n)} = \arg \min_{\mathbf{w} \in \Omega_w^{(n)}} \tilde{F}(\mathbf{w}; \mathbf{w}^{(n-1)}) + \sum_{l=1}^L \mathbf{w}_l^H \Psi_l \mathbf{w}_l \quad (30)$$

$$\text{Step 2) } \mathbf{u}^{(n)} = \arg \min_{\mathbf{u} \in \Omega_u^{(n)}} \mathbf{u}^H \mathbf{u} \quad (31)$$

where for notational simplicity, we define the projection of Ω onto each design block at the n^{th} iteration as $\Omega_w^{(n)} = \{\mathbf{w} : (\mathbf{w}, \mathbf{u}^{(n-1)}) \in \Omega\}$ and $\Omega_u^{(n)} = \{\mathbf{u} : (\mathbf{w}^{(n)}, \mathbf{u}) \in \Omega\}$. In Step 1), if we neglect the terms independent of \mathbf{w} in $\tilde{F}(\cdot; \cdot)$ and let $\lambda_d = \mu$, we observe that (30) becomes equivalent to the QCQP of (20). Furthermore, the solution to (31) is given by (15). Now we recognize that the proposed iteratively re-weighted algorithm in Algorithm 1 is essentially the above block-type MM algorithm, which solves the original optimization problem (6), however, with the aid of an approximated log-sum objective function.

Having established the above connection, we are ready to prove the convergence of Algorithm 1. To begin, let us first introduce the definition of the *Nash point* [23].

Definition 1: A point $(\bar{\mathbf{w}}, \bar{\mathbf{u}})$ is called a *Nash point* or *block coordinate-wise minimizer* of (28), if it satisfies the following Nash equilibrium conditions of (28):

$$\mathcal{F}'(\bar{\mathbf{w}}, \bar{\mathbf{u}}) \leq \mathcal{F}'(\mathbf{w}, \bar{\mathbf{u}}) \quad \forall \mathbf{w} \in \bar{\Omega}_w \quad (32a)$$

$$\mathcal{F}'(\bar{\mathbf{w}}, \bar{\mathbf{u}}) \leq \mathcal{F}'(\bar{\mathbf{w}}, \mathbf{u}) \quad \forall \mathbf{u} \in \bar{\Omega}_u, \quad (32b)$$

where $\bar{\Omega}_w \triangleq \{\mathbf{w} : (\mathbf{w}, \bar{\mathbf{u}}) \in \Omega\}$, and similarly, $\bar{\Omega}_u \triangleq \{\mathbf{u} : (\bar{\mathbf{w}}, \mathbf{u}) \in \Omega\}$.

Remark 2: In general, the Nash point of a non-convex optimization problem is a generalization of a stationary point. If the feasible set Ω is separable, i.e., Ω is a Cartesian product given by $\Omega = \Omega_w \times \Omega_u$ where Ω_w and Ω_u are two convex subsets, then the above Nash equilibrium conditions become equivalent to the first-order optimality conditions [24], and subsequently $(\bar{\mathbf{w}}, \bar{\mathbf{u}})$ becomes a stationary point. In view of this, the Nash equilibrium conditions are in general weaker than the first-order optimality conditions. For problem (28), a stationary point must be a Nash point, but a Nash point is not necessarily a stationary point. ■

With the above definition, the convergence properties of Algorithm 1 are formulated in the following theorem:

Theorem 1: Let $\{(\mathbf{w}^{(n)}, \mathbf{u}^{(n)})\}$ be the solution sequence generated by Algorithm 1. Then any limit point of $\{(\mathbf{w}^{(n)}, \mathbf{u}^{(n)})\}$ is a *Nash point* of problem (28), hence, satisfying the Nash equilibrium condition of (32).

Proof: The proof follows two steps. Firstly, we show that $\lim_{n \rightarrow \infty} \|\mathbf{w}^{(n)} - \mathbf{u}^{(n-1)}\|_2 = 0$ and $\lim_{n \rightarrow \infty} \|\mathbf{w}^{(n)} - \mathbf{w}^{(n-1)}\|_2 = 0$, the proof of which can be found in the Appendix. Then invoking [23, Theorem 2.3], it is readily shown that any limit point $(\bar{\mathbf{w}}, \bar{\mathbf{u}})$ of $\{(\mathbf{w}^{(n)}, \mathbf{u}^{(n)})\}$ is a Nash point of (36). ■

Before concluding this subsection, the following remark is of interest.

Remark 3 (On the convergence, optimality and uniqueness of the obtained solution): In the current state-of-the-art of the BCD algorithm [23], [27]–[30], there are in general two classes

of non-convex problems that this algorithm can efficiently solve, which are described below.² The first problem, denoted by (P_0) assumes the following form:

$$(P_0) : \quad \min_{\mathbf{x}} f(\mathbf{x}_1, \mathbf{x}_2) \quad \text{s.t. } \mathbf{x} = (\mathbf{x}_1, \mathbf{x}_2) \in \mathcal{X} \triangleq \mathcal{X}_1 \times \mathcal{X}_2$$

where $f : \mathbb{C}^{m_1} \times \mathbb{C}^{m_2} \rightarrow \mathbb{R}$ is a continuously differentiable function, and $\mathcal{X}_i \subseteq \mathbb{C}^{m_i}$, $i = 1, 2$ are closed, nonempty convex subsets. Let $\{\mathbf{x}^{(n)}\}$ denote the sequence of intermediate solutions generated by the BCD algorithm. Then it has been proved in [27]–[30] that every limit point of $\{\mathbf{x}^{(n)}\}$ is a stationary point of (P_0) .

Let us now proceed to a more general class of non-convex problems, to which our energy minimization problem belongs:

$$(P_1) : \quad \min_{\mathbf{x}} f(\mathbf{x}_1, \mathbf{x}_2) \quad \text{s.t. } \mathbf{x} \in \mathcal{X},$$

where $\mathcal{X} \subseteq \mathbb{C}^{m_1+m_2}$ is a closed and block multi-convex subset, i.e., \mathcal{X} is convex with respect to each of \mathbf{x}_1 and \mathbf{x}_2 , but not jointly convex in \mathbf{x} . In contrast to (P_0) , now \mathbf{x}_1 and \mathbf{x}_2 are nonlinearly coupled in the constraints and therefore the feasible set \mathcal{X} can no longer be expressed as a Cartesian product. The convergence behavior of the BCD algorithm for (P_1) has not been thoroughly investigated until very recently [23]. As a revelation, it has been proved in [23] that every limit point of $\{\mathbf{x}^{(n)}\}$ is a *Nash point* of (P_1) , provided that $f(\cdot)$ is strongly convex with respect to each of \mathbf{x}_1 and \mathbf{x}_2 .

Despite the elegant convergence properties of the BCD algorithm, it is worth noting that due to the non-convex nature of both (P_0) and (P_1) , there may exist many stationary or Nash points. At the time of writing, the question whether the algorithm converges to a unique stationary/Nash point remains an open issue in both the theoretical field of non-convex optimization [14], [23], [27]–[30] and in terms of its engineering applications [11], [31], [32]. Additionally, the local optimality of the solution obtained is not guaranteed. This is because for (P_0) , by the definition of a stationary point, it can either be a locally optimal point or a saddle point. For (P_1) , the current best effort is to prove the results in Theorem 1, where a Nash point is not necessarily a locally optimal point (see Definition 1). ■

C. RRH Selection and UE Admission Control

Upon the convergence of Algorithm 1, when a solution $(\bar{\mathbf{w}}, \bar{\mathbf{u}})$ is obtained, the *group sparsity pattern* associated with the set of RRHs' weight vectors can be retrieved by computing the squared norm of each RRH's weight vector, yielding

$$\mathcal{S} = [\mathcal{S}_1, \dots, \mathcal{S}_L] = [\|\bar{\mathbf{w}}_1\|_2^2, \dots, \|\bar{\mathbf{w}}_L\|_2^2] \quad (33)$$

where $\mathcal{S}_l \triangleq \|\mathbf{w}_l\|_2^2$ is used as a sparsity indicator for RRH- l . In contrast to prior works [5], [6], hereby we determine the subset \mathcal{A} consisting of the active RRHs in a single attempt by thresholding the sparsity indicator associated with each RRH. Specifically, we assume that when the sparsity indicator \mathcal{S}_l of RRH- l falls below a small threshold $\tau > 0$, RRH- l is switched

²To simplify the analysis, we limit our discussions on problems with two optimization variable blocks, i.e., \mathbf{x}_1 and \mathbf{x}_2 . However, all the results and discussions can be extended to the case of multi-block variables.

off for the sake of energy efficiency, and vice versa. In this way, we obtain

$$\mathcal{A} = \{l : \mathcal{S}_l \geq \tau, l \in \mathcal{L}\}. \quad (34)$$

Due to the reduced number of active RRHs participating in the relay-aided transmission, we have a reduced distributed diversity gain. Hence, the QoS constraints (6b) might be violated at some DUEs after deactivating selected RRHs. This infeasibility issue can be verified by reformulating (6) as a feasibility check problem. Specifically, only the subset \mathcal{A} of active RRHs is now involved in (6) instead of all the L RRHs and again, we can apply the concept of BCD update to solve the feasibility check problem. If a feasible solution is obtained, we subsequently further minimize the total transmission power of the active RRHs according to

$$\min_{\mathbf{w}, \mathbf{u}} \sum_{l \in \mathcal{A}} P_{t,l} \quad (35a)$$

$$\text{s.t. } \text{MSE}_k(u_k, \mathbf{w}) \leq \gamma_k \quad \forall k \in \mathcal{K} \quad (35b)$$

$$P_{t,l} \leq P_{l,\max} \quad \forall l \in \mathcal{A} \quad (35c)$$

$$\mathbf{w}_l = \mathbf{0} \quad \forall l \notin \mathcal{A}. \quad (35d)$$

Otherwise, if we fail to find a feasible solution, it becomes necessary to incorporate a mechanism which dynamically performs admission control for the end-users. A user admission control mechanism has been introduced in [34] for a multi-cell downlink scenario within a C-RAN, where the SINR is adopted as the QoS metric for each end-user. Following a similar design philosophy, hereby we propose a user admission control method for the multi-user relaying sub-network within C-RAN.

To this end, we introduce a real-valued vector $\mathbf{z} = [z_1, \dots, z_K]^T$, where z_k is an abstract measure of the extent to which the QoS constraint at DUE- k is violated. Motivated by the so-called phase-one method in [24], we can formulate the user admission control as the following feasibility problem:

$$\min_{\mathbf{u}, \mathbf{w}, \mathbf{z}} \mathbf{1}^T \mathbf{z} \quad (36a)$$

$$\text{s.t. } \sum_{l \in \mathcal{A}} \sum_{m \in \mathcal{A}} \mathbf{w}_l^H \mathbf{Q}_{l,m}^k \mathbf{w}_m - \sum_{l \in \mathcal{A}} 2\Re \{ \mathbf{w}_l^H \mathbf{q}_{k,l} \} + \sum_{l \in \mathcal{A}} \mathbf{w}_l^H \boldsymbol{\Theta}_{k,l} \mathbf{w}_l + q'_k \leq z_k, \quad k \in \mathcal{K} \quad (36b)$$

$$\mathbf{w}_l^H \boldsymbol{\Psi}_l \mathbf{w}_l \leq P_{l,\max}, \quad l \in \mathcal{A} \quad (36c)$$

$$\mathbf{z} \geq \mathbf{0} \quad (36d)$$

where $q'_k = q_k - \gamma_k$. The above problem is always feasible and can be reformulated as a convex SOCP. The infeasibility indicator $z_k = 0$ reveals that the k^{th} QoS constraint is satisfied, while $z_k > 0$ indicates the opposite. Therefore, all QoS constraints are satisfied if and only if $\mathbf{1}^T \mathbf{z} = 0$. Based on these observations, we then propose an iterative procedure to jointly check the feasibility and perform admission control, which is described by Algorithm 2. Specifically, at each iteration, we remove the specific DUE which has the highest infeasibility indicator, i.e., whose QoS constraint is the most ‘‘difficult’’ one

to satisfy. The procedure is repeated, until the QoS constraints for all the remaining DUEs are satisfied. This admission control procedure can be readily incorporated into the RRH relaying design at the BBU pool, which essentially solves the inherent infeasibility issue associated with the RRH selection.

IV. SIMULATION RESULTS

We evaluate the performance of the joint RRH selection and AF relay optimization algorithms proposed in Section III based on computer simulations. In all simulations, we assume that the channel coefficients are generated as independent and identically distributed (i.i.d.) complex circular Gaussian variables having a zero mean and a unit variance. For simplicity, all the RRHs are equipped with the same number of antennas N_l while the static power consumption $P_{c,l}$ and transmit power budget $P_{t,l}$ are both set to 0.5. The noise variances at the RRHs and the DUEs are respectively set to $\sigma_{R,l}^2 = 10^{-3}$ and $\sigma_{D,k}^2 = 10^{-2}$. The MSE target γ_k in (6) is defined in terms of the target SINR ρ , i.e., we have $\gamma_k = \frac{1}{\rho+1}$ for all $k \in \mathcal{K}$. Based on the observation that Algorithm 1 converges in about 10–15 iterations in all cases, Algorithm 1 is terminated after 20 iterations and $\varepsilon = 10^{-10}$ is adopted to avoid numerical instability. Each optimization problem in the form of (20) that is involved in Algorithms 1 and 2 is solved using the MATLAB-based interface YALMIP [35] along with the external solver MOSEK [36]. Each point or number in the subsequent figures and tables is obtained by averaging the results of 200 independent realizations. The above simulation parameters remain fixed unless otherwise stated. We compare the performance of the following algorithms:

- 1) The proposed joint RRH selection and relay optimization, which is labeled as ‘‘RRH Selection’’ (‘‘RRH Sel.’’);
- 2) The conventional collaborative relaying approach operating without RRH selection labeled as ‘‘w/o RRH Selection’’ (‘‘w/o RRH Sel.’’), whose objective is to minimize the total transmission power of all the RRHs in the absence of sparsity-inducing l_0 -norm [c.f. (6a)]. Mathematically, this problem can be written as

$$\min_{\mathbf{u}, \{\mathbf{W}_l\}} \sum_{l=1}^L P_{t,l} \quad (37a)$$

$$\text{s.t. } \text{MSE}_k(u_k, \{\mathbf{W}_l\}) \leq \gamma_k \quad \forall k \in \mathcal{K} \quad (37b)$$

$$P_{t,l} \leq P_{l,\max} \quad \forall l \in \mathcal{L}. \quad (37c)$$

We consider two simulation scenarios, namely, a generic relay sub-network and a heterogeneous network (HetNet).

A. Generic Relay Sub-Network

In Fig. 4, we show the total relaying sub-network’s power dissipation for the different methods as a function of the number of UE pairs K . A pair of multi-antenna settings, namely, one in which $N_l = 3$ for all l and one in which $N_l = 4$ for all l , are considered under three different target SINRs at the DUEs. Our results reveal that in general it is inefficient to allow all the RRHs to transmit data because this requires a significant amount of static power. However, the proposed algorithm is

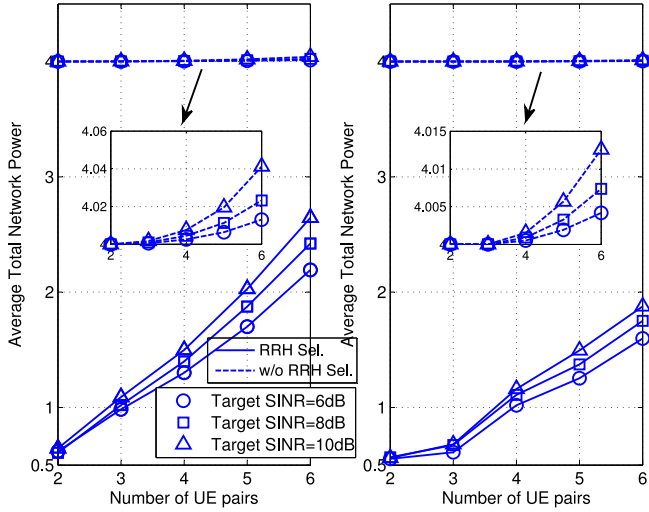


Fig. 4. Comparison of power consumption of the relaying sub-network using Algorithm 1 and of the one without RRH selection. (Left) $N_l = 3 \forall l$. (Right) $N_l = 4 \forall l$.

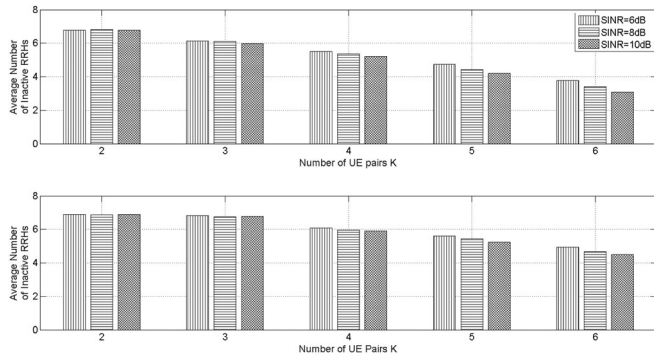


Fig. 5. Average number of inactive RRHs with different number of UE pairs K and target SINR ρ . (Top) $N_l = 3$. (Bottom) $N_l = 4$.

Algorithm 2: Iterative UE admission control algorithm.

Initialization: $\mathcal{K} = \{1, 2, \dots, K\}$;
while $1^T \bar{z} > 0$ **do**
 1) Solve the feasibility problem (36) considering the QoS constraints (36b) for $k \in \mathcal{K}$ and obtain \bar{z} as its solution;
 2) Set $\mathcal{K} = \mathcal{K} \setminus k$ where k corresponds to the largest \bar{z}_k among $\{\bar{z}_1, \dots, \bar{z}_K\}$
end

capable of adaptively selecting the most appropriate RRHs for relaying by exploiting the knowledge of the spatial channel at a given time instance. To gain a deeper insight into this approach, we calculate the average number of RRHs that are switched off during the iterative procedure for different setup, i.e., different K and N_l . The efficacy of the proposed algorithm becomes more evident from the corresponding results presented in Fig. 5, where on average 3 to 7 RRHs can be switched off for the sake of energy-efficient transmission.

TABLE I
 NUMBER OF NON-SCHEDULED DUES FOR DIFFERENT K AND TARGET SINR

Number of UE pairs K	6			8		
Target SINR ρ (dB)	6	8	10	6	8	10
Average number of excluded DUEs	0.06	0.32	0.34	1.06	1.20	1.83

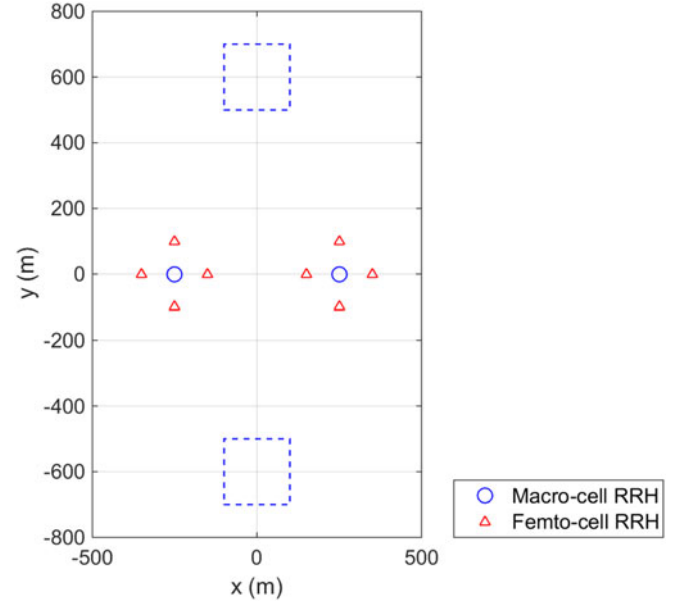


Fig. 6. Layout of the HetNet considered in the simulations.

Next, we examine the performance of the proposed DUE admission control mechanism in Algorithm 2. Hereby we adopt a more aggressive energy-efficient design method, where only a limited number of “dominant” RRHs remain active. To achieve this, upon recovering the sparsity pattern of the RRH weight vectors, i.e., \mathcal{S} in (33), we compute the average of the sparsity indicators, that is, $\bar{S} = \sum_{l=1}^L S_l / L$, and then determine the set of active RRHs as $\mathcal{A} = \{l : S_l \geq \eta \bar{S}, l \in \mathcal{L}\}$, where η is set to $\eta = 0.75$ in the simulations. In this way, the selected subset of active RRHs may not be capable of simultaneously maintaining an acceptable QoS at all DUEs. Then Algorithm 2 is invoked for iteratively removing the QoS constraints of specific DUEs from the optimization procedure. In Table I, the average number of non-scheduled (excluded) DUEs is listed for different number of UE pairs K and the target SINR ρ . It is clearly observed that the number of non-scheduled DUEs increases when more UEs requiring a higher QoS level are involved in the relay-assisted transmission.

B. HetNet Setup

In this subsection, we compare the performance of different methods in a HetNet setup, whose layout is sketched in Fig. 6. We consider a total of $L = 10$ RRHs, with two of them being macro-cell RRHs having a high power and the remaining ones are femto-cell RRHs having a relatively low power. A total of K SUEs are randomly deployed in the upper dashed line rectangle, whilst the corresponding K DUEs are randomly placed in the

TABLE II
SIMULATION PARAMETERS IN THE HETNET

Parameter	Value
Pathloss between macro-cell RRH and UE at distance d (km)	$128.1 + 37.6 \log_{10}(d)$
Pathloss between femto-cell RRH and UE at distance d (km)	$140.7 + 36.7 \log_{10}(d)$
Small-scale fading $\mathbf{h}_{l,k}$ and $\mathbf{g}_{k,l}$	Rayleigh fading
Noise power σ_R^2 and σ_D^2	-102 dBm
Static power $P_{c,l}$	5 W for macro RRHs and 3 W for femto RRHs
Transmission power for relay transmission $P_{l,\max}$	5W for all RRHs
Antenna gain	3 dBi

TABLE III
AVERAGE NUMBER OF INACTIVE (SILENT) RRHs FOR DIFFERENT SCHEMES

		Alg.	Num. of UE Pairs K			
			2	4	6	8
Relay Ant. Num. N_l	3	RRH Sel.	8.31	8	6.38	3.64
		w/o RRH Sel.	0	0	0	0
	4	RRH Sel.	8.80	8.40	7.96	6.11
		w/o RRH Sel.	0	0	0	0

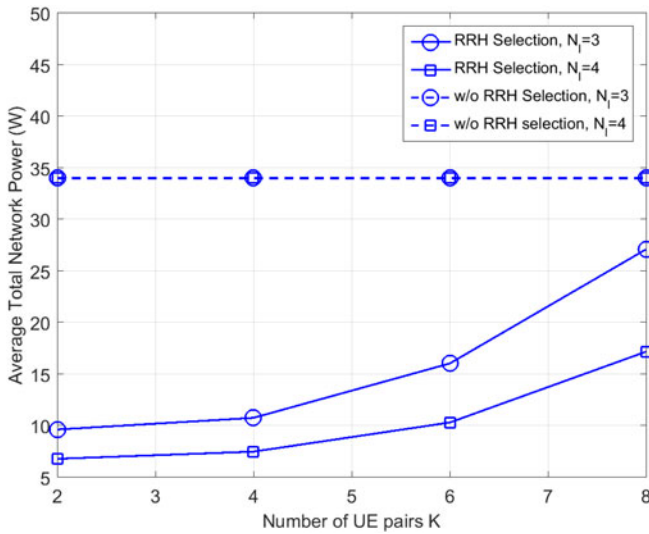


Fig. 7. Average network power consumption versus the number of UE pairs in a HetNet.

lower dashed line rectangle, based on the uniform distribution. The specific system parameters characterizing the HetNet are summarized in Table II, where asymmetric pathloss models are considered for different types of RRHs. The performance of different methods is compared in terms of the average total network power and the number of inactive RRHs.

In Fig. 7, the average network power consumption is shown as a function of the number of UE pairs K . Two different antenna array configurations are considered at the RRHs, namely, $N_l = 3$ and $N_l = 4$ for all $l \in \mathcal{L}$. It is observed that the proposed RRH selection achieves a significantly better energy efficiency than the conventional approach operating without RRH selection. Specifically, the performance gap is more evident,

when the number of UEs is relatively small. When more UEs are involved in the transmission, the gap between the two approaches is reduced. This is because a large portion of the *spatial diversity gain* provided by the multiple RRHs' antenna arrays must be exploited to serve the additional end-users, hence more RRHs remain active in the relay-aided transmission. For a similar reason, the power consumption becomes lower, when additional antennas are employed at the RRHs, yielding a saving of about 35% for the case of $K = 6$ and 40% for the case of $K = 8$. The numbers of inactive RRHs in the HetNet using the two different approaches are shown in Table I. For the case of $N_l = 3$, our proposed method yields a range of 3–8 inactive RRHs, whilst the numbers become 6–9 for the case of $N_l = 4$.

In summary, all the simulation results demonstrate the benefits of the proposed joint AF relaying optimization and RRH selection algorithm. In both generic relaying and heterogeneous network scenarios, the proposed method yields a significantly higher level of energy efficiency than that of its counterpart operating without RRH selection.

V. CONCLUSIONS

The problem of joint RRH relay selection and AF matrices design was investigated from a network energy minimization perspective for a multi-antenna multi-user relaying sub-network within a C-RAN. Relying on the so-called re-weighted l_1 minimization and BCD-type methods, an iterative algorithm having a proven convergence was proposed for solving the original non-convex optimization problem. Based on the recovered *group sparsity pattern* associated with the RRHs' AF matrices, the set of active RRHs involved was then determined. To overcome the inherent infeasibility issue of the RRH selection, an iterative end-user admission control algorithm was proposed, which can be readily incorporated into the relaying optimization at the BBU pool. Our simulation results demonstrated the efficacy of the proposed algorithms, which significantly reduced the energy consumption of the C-RAN over that of a conventional cooperative relaying approach.

APPENDIX

PROOF OF THE FIRST STEP IN THEOREM 1

We have to show that the sequence $\{(\mathbf{w}^{(n)}, \mathbf{u}^{(n)})\}$ is a square summable sequence such that $\lim_{n \rightarrow \infty} \|\mathbf{w}^{(n)} - \mathbf{w}^{(n-1)}\|_2^2 = 0$ and $\lim_{n \rightarrow \infty} \|\mathbf{u}^{(n)} - \mathbf{u}^{(n-1)}\|_2^2 = 0$. Based on the majorization relation in (29), we have

$$\begin{aligned}
 \mathcal{F}(\mathbf{w}^{(n)}) &+ \sum_{l=1}^L \mathbf{w}_l^{(n)H} \Psi_l \mathbf{w}^{(n)} + \mathbf{u}^{(n)H} \mathbf{u}^{(n)} \\
 &\leq \tilde{\mathcal{F}}(\mathbf{w}; \mathbf{w}^{(n-1)}) + \sum_{l=1}^L \mathbf{w}_l^{(n)H} \Psi_l \mathbf{w}^{(n)} + \mathbf{u}^{(n)H} \mathbf{u}^{(n)} \\
 &\leq \mathcal{F}(\mathbf{w}^{(n-1)}) + \mathcal{G}(\mathbf{w}^{(n-1)}) \\
 &\quad - \frac{\tau(\mathbf{w})}{2} \|\mathbf{w}^{(n)} - \mathbf{w}^{(n-1)}\|_2^2 - \frac{\tau(\mathbf{u})}{2} \|\mathbf{u}^{(n)} - \mathbf{u}^{(n-1)}\|_2^2
 \end{aligned} \tag{38}$$

where the first inequality is due to the majorization relation in (29) while the second inequality results from $\mathcal{F}(\mathbf{w}^{(n-1)}) = \mathcal{F}(\mathbf{w}; \mathbf{w}^{(n-1)})$ and the strong convexity of $\sum_{l=1}^L \mathbf{w}_l^H \Psi_l \mathbf{w}$ and $\mathbf{u}^H \mathbf{u}$ with parameters $\tau(\mathbf{w}) > 0$ and $\tau(\mathbf{u}) > 0$, respectively. Then summing the above inequality over n from 0 to \bar{n} , we arrive at

$$\begin{aligned} & \mathcal{F}(\mathbf{w}^{(0)}) + \sum_{l=1}^L \mathbf{w}_l^{(0)H} \Psi_l \mathbf{w}^{(0)} + \mathbf{u}^{(0)H} \mathbf{u}^{(0)} \\ & - \left(\mathcal{F}(\mathbf{w}^{(\bar{n})}) + \sum_{l=1}^L \mathbf{w}_l^{(\bar{n})H} \Psi_l \mathbf{w}^{(\bar{n})} + \mathbf{u}^{(\bar{n})H} \mathbf{u}^{(\bar{n})} \right) \\ & \geq \sum_{n=0}^{\bar{n}} \left(\frac{\tau(\mathbf{w})}{2} \|\mathbf{w}^{(n)} - \mathbf{w}^{(n-1)}\|_2^2 + \frac{\tau(\mathbf{u})}{2} \|\mathbf{u}^{(n)} - \mathbf{u}^{(n-1)}\|_2^2 \right). \end{aligned} \quad (39)$$

It is not difficult to observe that the objective function in (28) is monotonically decreasing after each iteration and lower bounded at least by zero, so that the left-hand side of the above equation is a finite positive number. Upon letting $\bar{n} \rightarrow \infty$, we therefore conclude that $\lim_{n \rightarrow \infty} \|\mathbf{w}^{(n)} - \mathbf{w}^{(n-1)}\|_2^2 = 0$ and $\lim_{n \rightarrow \infty} \|\mathbf{u}^{(n)} - \mathbf{u}^{(n-1)}\|_2^2 = 0$.

ACKNOWLEDGMENT

The authors would like to thank the Editor and the anonymous reviewers for their valuable comments, which have helped to improve the quality and the presentation of this paper.

REFERENCES

[1] N. Zhang, N. Cheng, A. T. Gamage, K. Zhang, J. W. Mark, and X. Shen, "Cloud assisted HetNets toward 5G wireless networks," *IEEE Commun. Mag.*, vol. 53, no. 6, pp. 59–65, Jun. 2015.

[2] B. Soret, K. I. Pedersen, N. T. K. Jørgensen, and V. Fernández-López, "Interference coordination for dense wireless networks," *IEEE Commun. Mag.*, vol. 53, no. 1, pp. 102–109, Jan. 2015.

[3] "C-RAN: The road towards green RAN," *China Mobile Research Institute*, Beijing, China, White paper, ver. 2.5, Oct. 2011.

[4] M. Peng, Y. Sun, X. Li, Z. Mao, and C. Wang, "Recent advances in cloud radio access networks: System architectures, key techniques, and open issues," *IEEE Commun. Surveys Tut.*, vol. 18, no. 3, pp. 2282–2308, Third Quarter 2016.

[5] Y. Shi, J. Zhang, and K. B. Letaief, "Group sparse beamforming for green cloud-RAN," *IEEE Trans. Wireless Commun.*, vol. 13, no. 5, pp. 2809–2823, May 2014.

[6] Y. Shi, J. Zhang, and K. B. Letaief, "Robust group sparse beamforming for multicast green cloud-RAN with imperfect CSI," *IEEE Trans. Signal Process.*, vol. 63, no. 17, pp. 4647–4659, Sep. 2015.

[7] S. Luo, R. Zhang, and T. J. Lim, "Downlink and uplink energy minimization through user association and beamforming in C-RAN," *IEEE Trans. Wireless Commun.*, vol. 14, no. 1, pp. 494–508, Jan. 2015.

[8] B. Dai and W. Yu, "Sparse beamforming and user-centric clustering for downlink cloud radio access network," *IEEE Access*, vol. 2, pp. 1326–1339, Oct. 2014.

[9] Y. Shi, J. Zhang, K. B. Letaief, B. Bai, and W. Chen, "Large-scale convex optimization for ultra-dense cloud-RAN," *IEEE Wireless Commun.*, vol. 22, no. 3, pp. 84–91, Jun. 2015.

[10] Y. Rong, X. Tang, and Y. Hua, "A unified framework for optimizing linear nonregenerative multicarrier MIMO relay communication systems," *IEEE Trans. Signal Process.*, vol. 57, no. 12, pp. 4837–4851, Aug. 2009.

[11] C. Xing, S. Ma, and Y.-C. Wu, "Robust joint design of linear relay precoder and destination equalizer for dual-hop amplify-and-forward MIMO relay systems," *IEEE Trans. Signal Process.*, vol. 58, no. 4, pp. 2273–2283, Apr. 2010.

[12] O. Arnold, F. Richter, G. Fettweis, and O. Blume, "Power consumption modeling of different base station types in heterogeneous cellular networks," in *Proc. Future Netw. Mobile Summit*, Florence, Italy, Jun. 2010, pp. 1–8.

[13] E. J. Candès, M. B. Wakin, and S. P. Boyd, "Enhancing sparsity by reweighted l_1 minimization," *J. Fourier Anal. Appl.*, no. 13, pp. 877–905, Oct. 2008.

[14] D. P. Bertsekas, *Nonlinear Programming*, 2nd ed. Singapore: Athena Scientific, 1999.

[15] M. R. A. Khandaker and Y. Rong, "Interference MIMO relay channel: Joint power control and transceiver-relay beamforming," *IEEE Trans. Signal Process.*, vol. 60, no. 12, pp. 6509–6518, Dec. 2012.

[16] K. T. Truong, P. Sartori, and R. W. Heath, "Cooperative algorithms for MIMO amplify-and-forward relay networks," *IEEE Trans. Signal Process.*, vol. 61, no. 5, pp. 1272–1287, Mar. 2013.

[17] J. Yang and B. Champagne, "Joint transceiver optimization for MIMO multiuser relaying networks with channel uncertainties," in *Proc. IEEE 80th Veh. Technol. Conf.*, Vancouver, BC, Canada, Sep. 2014, pp. 1–6.

[18] J. Yang, Y. Cai, B. Champagne, and L. Hanzo, "Multi-user beamforming-aided AF relaying: A low-complexity adaptive design approach," in *Proc. Asilomar Conf. Signals Sys. Comput.*, Pacific Grove, CA, Nov. 2015, pp. 983–988.

[19] J. Yang, B. Champagne, Y. Zou, and L. Hanzo, "Joint optimization of transceiver matrices for MIMO-aided multiuser AF relay networks: Improving the QoS in the presence of CSI errors," *IEEE Trans. Veh. Technol.*, vol. 65, no. 3, pp. 1434–1451, Mar. 2016.

[20] H. Ning, C. Ling, and K. K. Leung, "Relay-aided interference alignment: Feasibility conditions and algorithm," in *Proc. IEEE Int. Sym. Inf. Theory*, Austin, TX, Jun. 2010, pp. 390–394.

[21] B. Nourani, S. A. motahari, and A. K. Khandani, "Relay-aided interference alignment for the quasi-static interference channel," in *Proc. IEEE Int. Symp. Inf. Theory*, Austin, TX, Mar. 2010, pp. 405–409.

[22] K. P. Murphy, *Machine Learning: A Probabilistic Perspective*. Cambridge, MA: MIT Press, 2012.

[23] Y. Xu and W. Yin, "A block coordinate descent method for regularized multiconvex optimization with applications to nonnegative tensor factorization and completion," *SIAM J. Imaging Sci.*, vol. 6, no. 3, pp. 1758–1789, Sep. 2013.

[24] S. Boyd and L. Vandenberghe, *Convex Optimization*. Cambridge, U.K.: Cambridge Univ. Press, 2004.

[25] M. S. Lobo, L. Vandenberghe, S. Boyd, and H. Lebret, "Applications of second-order cone programming," *Linear Algebra Appl.*, vol. 284, no. 1–3, pp. 193–228, Nov. 1998.

[26] J. Löfberg, YALMIP Wiki: Solvers. [Online]. Available: <http://users.isy.liu.se/johanl/yalmip/pmwiki.php?n=Solvers.Solvers>

[27] A. Beck and L. Tretuashvili, "On the convergence of block coordinate descent type methods," *SIAM J. Control Optim.*, vol. 23, no. 4, pp. 2037–2060, 2013.

[28] P. Tseng, "Convergence of a block coordinate descent method for non-differentiable minimization," *J. Optim. Theory Appl.*, vol. 109, no. 3, pp. 475–494, Jun. 2001.

[29] Z.-Q. Luo and P. Tseng, "On the convergence of the coordinate descent method for convex differentiable minimization," *J. Optim. Theory Appl.*, vol. 72, no. 1, pp. 7–35, Jan. 1992.

[30] M. Razaviyayn, M. Hong, and Z.-Q. Luo, "A unified convergence analysis of block successive minimization methods for nonsmooth optimization," *SIAM J. Optim.*, vol. 23, no. 2, pp. 1126–1153, 2013.

[31] Z. Qin, K. Scheinberg, and D. Glodfarb, "Efficient block-coordinate descent algorithms for the group lasso," *Math. Program. Comput.*, no. 5, pp. 143–169, 2013.

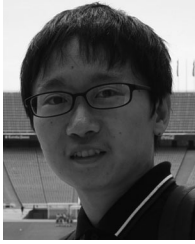
[32] Q. Li *et al.*, "Transmit solutions for MIMO wiretap channels using alternating optimization," *IEEE J. Sel. Areas Commun.*, vol. 31, no. 9, pp. 1714–1727, Sep. 2013.

[33] D. R. Hunter and K. Lange, "A tutorial on MM algorithms," *Amer. Stat.*, vol. 58, no. 1, pp. 30–37, Feb. 2004.

[34] Y. Shi, J. Cheng, J. Zhang, B. Bai, W. Chen, and K. B. Letaief, "Smoothed l_p -minimization for green cloud-RAN with user admission control," *IEEE J. Sel. Areas Commun.*, vol. 34, no. 4, pp. 1022–1036, Apr. 2016.

[35] J. Löfberg, "YALMIP: A toolbox for modeling and optimization in MATLAB," in *Proc. IEEE Int. Symp. Comput. Aided Control Syst. Design*, Taipei, Taiwan, Sep. 2004, pp. 284–289.

[36] E. D. Andersen and K. D. Andersen, *MOSEK Modeling Manual*. Aug. 2013. [Online]. Available: <http://mosek.com>



Jiaxin Yang (S'11) received the B.Eng. degree in information engineering from Shanghai Jiao Tong University, Shanghai, China, in 2009 and the M.E.Sc. degree in electrical and computer engineering from the University of Western Ontario, London, ON, Canada, in 2011. Since September 2012, he has been with the Department of Electrical and Computer Engineering, McGill University, Montreal, QC, Canada, where he is currently working towards the Ph.D. degree. His research interests include optimization theory, statistical signal processing, detection and estimation, and

the applications thereof in wireless communications such as MIMO systems, cooperative communications, and physical-layer security. Since December 2015, he has been a Wireless Research Consultant at InterDigital Canada, Montreal. He has received several awards and scholarships, including the Best Paper Award of 27th IEEE International Symposium on Personal, Indoor, and Mobile Radio Communications; the McGill Engineering Doctoral Award, the Graduate Excellence Fellowship; the International Differential Tuition Fee Waivers; the FRQNT International Internship Scholarship; the PERSWADE Ph.D. Scholarship; the Graduate Research Enhancement and Travel Awards; and the Graduate Research Mobility Awards.



Benoit Champagne (S'87–M'89–SM'03) received the B.Eng. degree in engineering physics from the École Polytechnique de Montréal, Montreal, QC, Canada, in 1983; the M.Sc. degree in physics from the Université de Montréal in 1985; and the Ph.D. degree in electrical engineering from the University of Toronto, Toronto, ON, Canada, in 1990. From 1990 to 1999, he was an Assistant Professor and then Associate Professor with INRS-Telecommunications, Université du Québec, Montréal. In 1999, he joined McGill University, Montreal, where he is now a Full

Professor within the Department of Electrical and Computer Engineering. He served as Associate Chairman of graduate studies in the department from 2004 to 2007. His research focuses on the study of advanced algorithms for the processing of information bearing signals by digital means. His interests span many areas of statistical signal processing, including detection and estimation, sensor array processing, adaptive filtering, and applications thereof to broadband communications and audio processing, where he has co-authored more than 200 referred publications. His research has been funded by the Natural Sciences and Engineering Research Council (NSERC) of Canada, the "Fonds de Recherche sur la Nature et les Technologies" from the Government of Quebec, as well as some major industrial sponsors, including Nortel Networks, Bell Canada, InterDigital, and Microsemi. He has been an Associate Editor of the IEEE SIGNAL PROCESSING LETTERS, the IEEE TRANSACTIONS ON SIGNAL PROCESSING, and the *EURASIP Journal on Applied Signal Processing*. He has also served on the Technical Committees of several international conferences in the fields of communications and signal processing. In particular, he was a Co-Chair, Wide Area Cellular Communications Track, for the IEEE International Symposium on PIMRC (Toronto, Sep. 2011), Co-Chair, Antenna and Propagation Track, for the IEEE VTC-Fall, (Los Angeles, CA, USA, Sep. 2004), and Registration Chair for the IEEE International Conference on ASSP (Montreal, May 2004).



Yulong Zou (SM'13) received the B.Eng. degree in information engineering from the Nanjing University of Posts and Telecommunications (NUPT), Nanjing, China, in July 2006; the first Ph.D. degree in electrical engineering from the Stevens Institute of Technology, Hoboken, NJ, USA, in May 2012; and the second Ph.D. degree in signal and information processing from NUPT in July 2012. He is currently a Professor at NUPT. His research interests span a wide range of topics in wireless communications and signal processing, including cooperative communications, cognitive radio, wireless security, and energy-efficient communications.

Dr. Zou received the 2014 IEEE Communications Society Asia-Pacific Best Young Researcher award. He serves on the editorial board of IEEE COMMUNICATIONS SURVEYS AND TUTORIALS, IEEE COMMUNICATIONS LETTERS, *IET Communications*, and the *EURASIP Journal on Advances in Signal Processing*. In addition, he has acted as symposium chair, session chair, and TPC member for a number of IEEE sponsored conferences, including the IEEE Wireless Communications and Networking Conference (WCNC), IEEE Global Communications Conference (GLOBECOM), IEEE International Conference on Communications (ICC), IEEE Vehicular Technology Conference (VTC), International Conference on Communications in China (ICCC), and so on.



Lajos Hanzo (M'91–SM'92–F'04) received the degree in electronics in 1976 and the Doctorate degree in 1983. In 2009, he received an honorary doctorate degree from the Technical University of Budapest, Hungary, and in 2015 from the University of Edinburgh, U.K. During his 40-year career in telecommunications, he has held various research and academic posts in Hungary, Germany, and the U.K. Since 1986, he has been with the School of Electronics and Computer Science, University of Southampton, Southampton, U.K., where he holds the Chair in telecommunications.

He has successfully supervised more than 100 Ph.D. students, co-authored 18 Wiley/IEEE Press books on mobile radio communications, totalling in excess of 10 000 pages, published 1641 research entries on IEEE Xplore, acted both as TPC and General Chair of IEEE conferences, presented keynote lectures, and has been awarded a number of distinctions. He is currently directing a 60-strong academic research team, working on a range of research projects in the field of wireless multimedia communications sponsored by industry, the Engineering and Physical Sciences Research Council (EPSRC) U.K., the European Research Council's Advanced Fellow Grant, and the Royal Society's Wolfson Research Merit Award. He is an enthusiastic supporter of industrial and academic liaison, and he offers a range of industrial courses. He is also a Governor of the IEEE VTS. During 2008–2012, he was the Editor-in-Chief of the IEEE Press and a Chaired Professor also at Tsinghua University, Beijing, China. His research is funded by the European Research Council's Senior Research Fellow Grant. He is a Fellow of Royal Academy of Engineering, IET, and EURASIP. For further information on research in progress and associated publications please refer to <http://www-mobile.ecs.soton.ac.uk>. He has 30 000+ citations.